3-D seismic imaging of complex intrusions

Hans-Henrik Westbroek and Robert R. Stewart

ABSTRACT

The goal of this research is to assess the feasibility of using 3-D seismology for the prospecting and delineation of ore bodies. Since 3-D seismic surveying has been successfully used to define many complicated geologic structures in the oil and gas industry, it would seem to be a very promising survey for hard rock environments. Due to the complexity of the structure, accurate migration of the data is critical for proper interpretation. The initial phase of this research is to compare 2-D and 3-D migration techniques on physical modeling data obtained from an extremely rugose target.

A copper nugget was used as the target. The data obtained from the model showed many strong, heavily scattered reflections from the surface of the nugget. 2-D migration proved to be quite successful in delineating the bulk dimensions of the nugget and showing the surface profile. We anticipate that the 3-D migration will provide a more accurate image especially in terms of detail along the surface of the nugget. More structural information will be attained by taking time slices through the 3-D data volume.

INTRODUCTION

Common geophysical techniques used in the prospecting for ore bodies include magnetic, EM, gravity, resistivity and IP methods (Dobrin, 1976) as many ore bodies are characterized by high conductivity, high density, and high magnetic susceptibility because of the presence of magnetite as an associated or marker mineral. However, these methods are not always applicable as some ore zones are associated with structure which remains hidden by highly conductive overburden (Hearst et al., 1994). Furthermore, non-seismic methods may not provide accurate or unique images at the depths now required for mining.

Seismic reflection surveys have played a large role in the exploration and development of hydrocarbons in the oil and gas industry. With the use of 3-D reflection seismic techniques, complex geological structures have been better resolved resulting in greater drilling success (Nestvold, 1992; Greenlee et al., 1994). It would seem, then, that 3-D seismic might have the same potential to resolve complex structure associated with intrusives and other geological settings in which ore bodies are found. Of course, seismic reflection surveys can only be effective where there is an appreciable variation in acoustic impedance such that reflections occur. Noponen (1979) demonstrated that this is true for crystalline rocks. In fact 2-D seismic surveying has already proven to be successful in these less traditional geological environments for seismic exploration.

One of the first vibroseis reflection surveys at a mine site in North America was conducted at the Buchans mine in Newfoundland (Thurlow et al., 1992). The ore bodies consist of polymetallic sulfide deposits in a stratigraphic sequence of volcanogenic felsic pyroclastic rocks which was structurally repeated many times by thrust faults. In this case, the seismic survey provided a cost-effective means to obtain valuable knowledge of the Buchans structure. Direct detection of massive sulfide bodies has been attempted as well (Fais et al., 1991; Hearst et al., 1994). The Fais et al. (1991) experiment was quite successful (Figure 1) while Hearst et al. (1994) met with limited success due in part to acquisition problems precipitated by extreme weather conditions.

Seismic surveys have also been used to help in the development of mine works. This is especially true in the coal industry where seismic surveys are primarily used for mine planning and safety rather than for the exploration of new coal fields (Gochioco, 1990; Lambourne et al., 1991). Seismic surveys have also been taken completely underground in a potash mine for this purpose (Gendzwill, 1993).

2-D seismic surveying is already prevalent as a technique for mineral prospecting so it would seem that the next logical step is the investigation and application of 3-D techniques for better refinement of complex structure. This paper is a first step in this investigation by studying the resolving capabilities of 3-D migration versus 2-D migration for a complex target. This investigation is simplified by using a data set which was collected over a rugose target submerged in water.

DATA ACQUISITION

Acquisition of the data was performed in a small physical modeling tank. A copper nugget, approximately 23 cm by 13.5 cm was used as the target (Figure 2). Figure 3 shows a schematic of the model setup including the tank, nugget and image area. The scale of the modeling tank is 1:10000. The acquisition parameters are listed in table 1. The survey was run in a single offset mode whereby the source and receiver were placed next to each other in the inline direction and stepped to each station where a shot was recorded. To improve the signal-to-noise ratio, each shot was stacked 32 times. This resulted in a 100% single-fold single-offset dataset. PVC foam was used to line the bottom of the tank in an attempt to lessen the effect of bottom reverberation.

ACQUISITION PARAMETERS	
Source	Parametrics transducer (1MHz)
Receiver	Parametrics transducer (1MHz)
Station Spacing	20m
Line Spacing	20m
No. of Inline Traces	100
No. of Crossline Traces	180
Sample Rate	1ms
No. Samples per Trace	2000
Bin Size	20m by 20m
Shot Stacking	32
Offset	220m
Dataset size (SEG-Y)	148 MB

TABLE 1. Survey acquisition parameters scaled to field dimensions.

PROCESSING

The processing flow is relatively simple and includes application of the proper shooting geometry, correction for spherical divergence, NMO correction to true zero-offset and migration (Figure 4). The relevant medium velocities are listed in Table 2.

Spherical divergence compensates for the geometric spreading of the source energy from the shot point. NMO is applied to correct the data for the single offset moveout. The data is then migrated in a 2-D and 3-D sense and displayed. Various lines within the dataset are compared before and after the migration algorithms have been applied. The 3-D migrated result will also be analyzed via an interpretation package for structure and time slices of the 3-D volume.

Figures 5 and 6 show Inline 90 and Crossline 50 as representative seismic lines from the raw data. Both are lines that run directly over the middle of the nugget. The extent of scatter is easily seen. Figures 7 and 8 show the same sections respectively after a 2-D migration algorithm has been applied. Note that the result gives good bulk dimensions of the nugget (length, width and height) as compared to the actual measured dimensions. The 3-D migrated results have yet to be produced for comparison.

Medium	Velocity (m/s)
Water	1498
Copper	4658
PVC foam	984

TABLE 2. Relevant medium velocities used for processing.

CONCLUSIONS

The 2-D time migration algorithm applied to the two representative lines worked well in determining the dimensions of the nugget. However, we anticipate that the 3-D migrated results will provide better results especially when time slices are provided of the data volume.

FUTURE WORK

The final stages of processing as described above will be completed shortly. Further research in this area will include similar studies on more realistic geologic models such as kimberlite pipes. Turning-ray migration may be useful in imaging the sides of these carrot-shaped structures. Full elastic 3D seismic surveying will be utilized in these studies. We also hope to acquire some real data for processing and interpretation.

ACKNOWLEDGMENTS

We wish to extend our thanks to Mr. Eric Gallant for setting up the physical model and collecting the data. Our appreciation to Mr. Glenn Larson and Mr. Mark Lane for their helpful discussions during processing and preparation of this document.

REFERENCES and FURTHER READING

Dobrin, M.B., 1976, Introduction to geophysical prospecting, 3rd Ed., McGraw Hill.

Doyle, H.A., 1990, Geophysical exploration for gold - A review, Geophysics, **55**, 2, p. 134-146.

Fais, S., Porceddu, E. and Tocco, R., 1991, High-resolution seismic reflection survey of a massive sulfide orebody in Sardinia, Italy - An experiment, Ore Geology Reviews, **6**, 1, p. 1-8.

Gendzwill, D.J. and Brehm, R., 1993, High-resolution seismic reflections in a potash mine, Geophysics, **58**, 5, p. 741-748.

Greenlee, S.M., Gaskins, G.M. and Johnson, M.G., 1994, 3-D seismic benefits from exploration through development: An Exxon perspective, The Leading Edge, July, p. 730-734.

Gochioco, L.M., 1990, Seismic surveys for coal exploration and mine planning, Geophysics: The Leading Edge of Exploration, **9**, 4, p. 25-28.

Hearst, R.B., Morris, W.A. and Scheick, D.G., 1994, Reflection seismic profiling for massive sulphides in the Arctic, 64th Annual Meeting of the S.E.G., Technical Program Expanded Abstracts With Authors' Biographies, p. 531-533.

Lambourne, A.N., Hatherly, P.J. and Evans, B.J., 1991, 3D Seismic Reflection: Examples of its Application to Mine Planning and Safety in Australian Coalfields, Exploration Geophysics, **22**, 1, p. 227-230.

Milkereit, B., Stumpel, H. and Rabbel W., 1986, Shear-wave reflection profiling for near-surface lignite exploration, Geophysical Prospecting, **34**, p. 845-855.

Nestvold, E.O., 1992, 3-D Seismic: Is the promise fulfilled?, Geophysics: The Leading Edge of Exploration, June, p. 12-19.

Noponen, I., Heikkinen, P. and Mehrotra S., 1979, Applicability of Seismic Reflection Sounding In Regions of PreCambrian Geology, Geoexploration **17**, p. 1-9.

Thurlow, J.G. et. al., 1992, Geological interpretation of a high resolution seismic survey at Buchans mine, Newfoundland, Can. J. Earth Sci., **29**, p. 2022-2037.

Yilmaz, O., 1987, Seismic data processing, SEG Investigations in Geophysics, Volume 2.

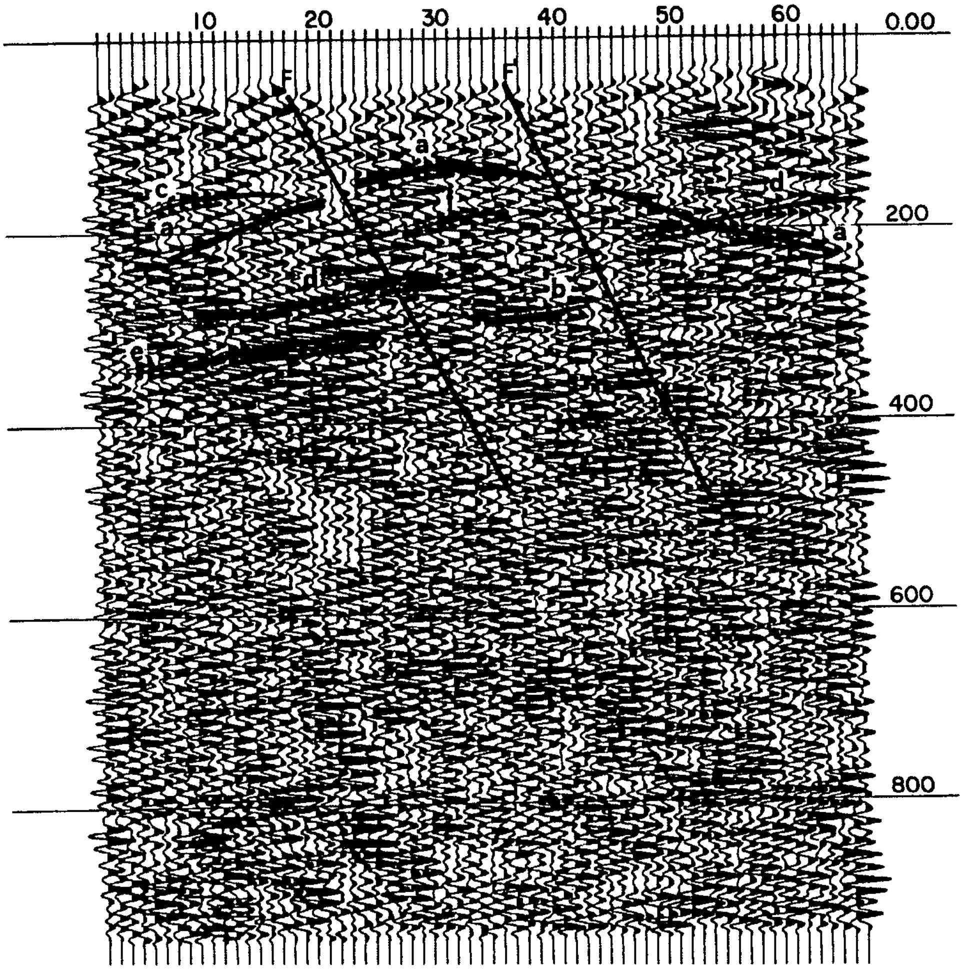

FIG. 1. Interpreted section from experimental survey showing top of the sulfide orebody at *a*, bottom of the orebody at *b* and fracture zones *F* and *F'*. The other reflectors labelled *c*, *d* and *f* are discussed in the text of Fais' (1991) paper.

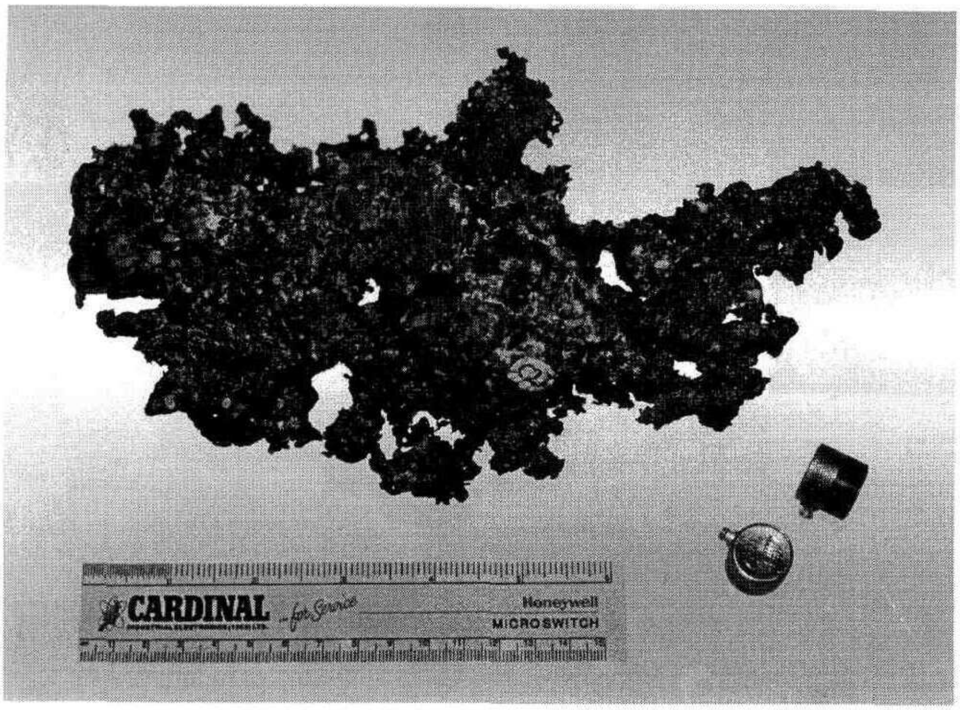

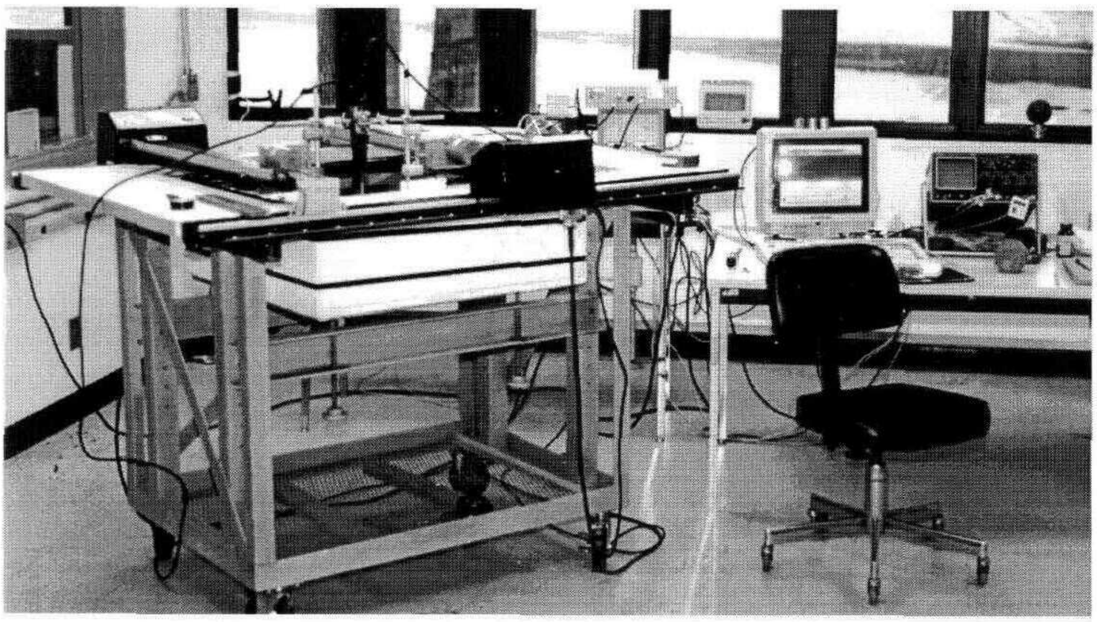

FIG. 2. Photograph of the copper nugget with transducers (top) and physical modeling tank set-up (bottom).

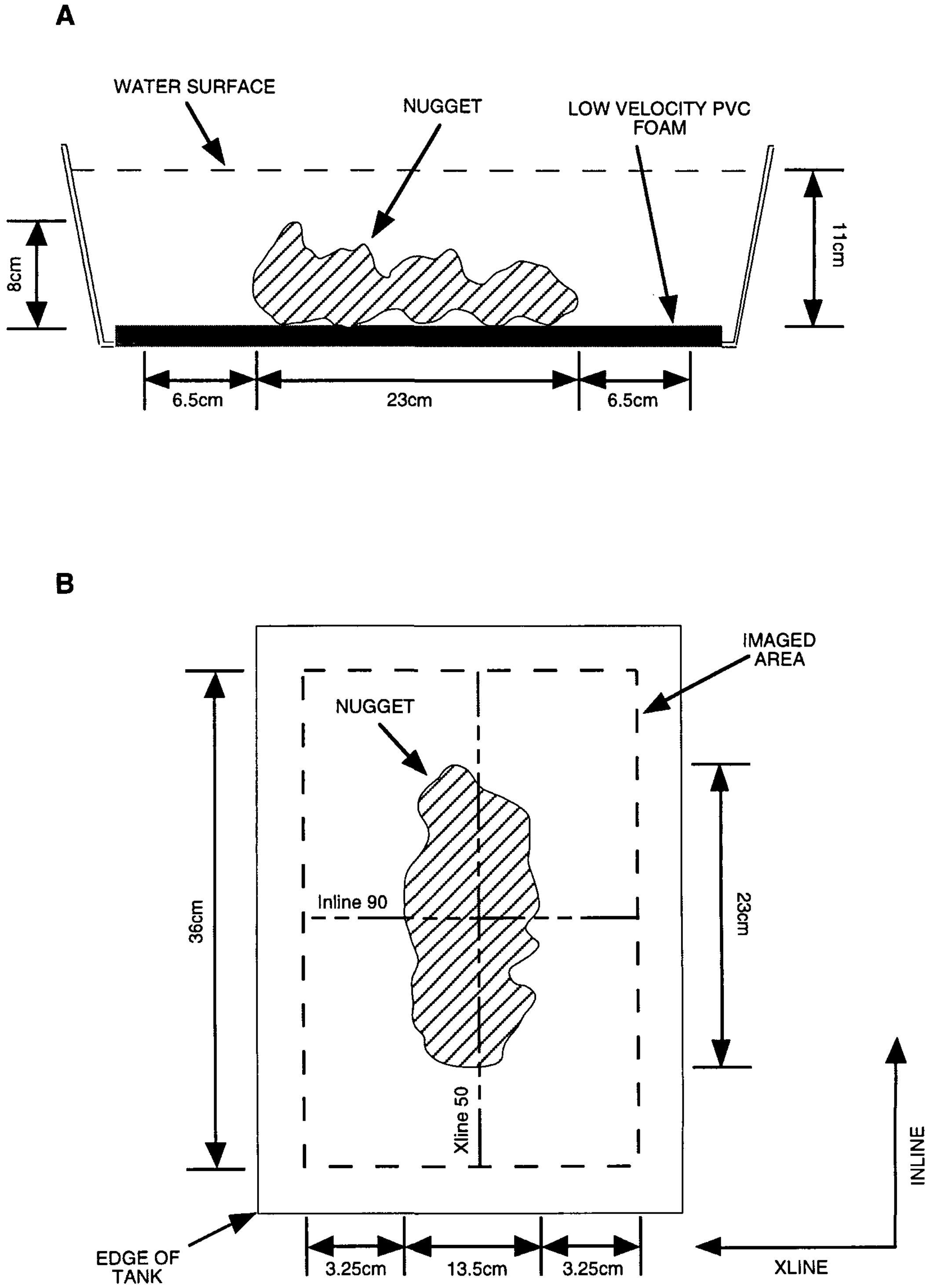

FIG. 3. Schematic diagram showing the acquisition set-up and actual dimensions in crossection (A) and plan view (B).

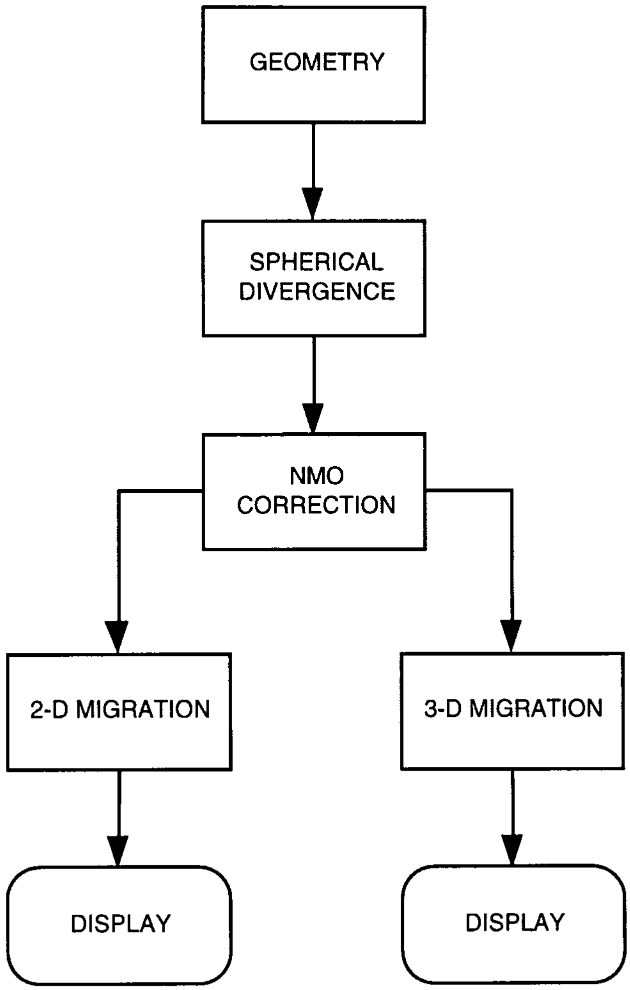

FIG. 4. Basic processing flow.

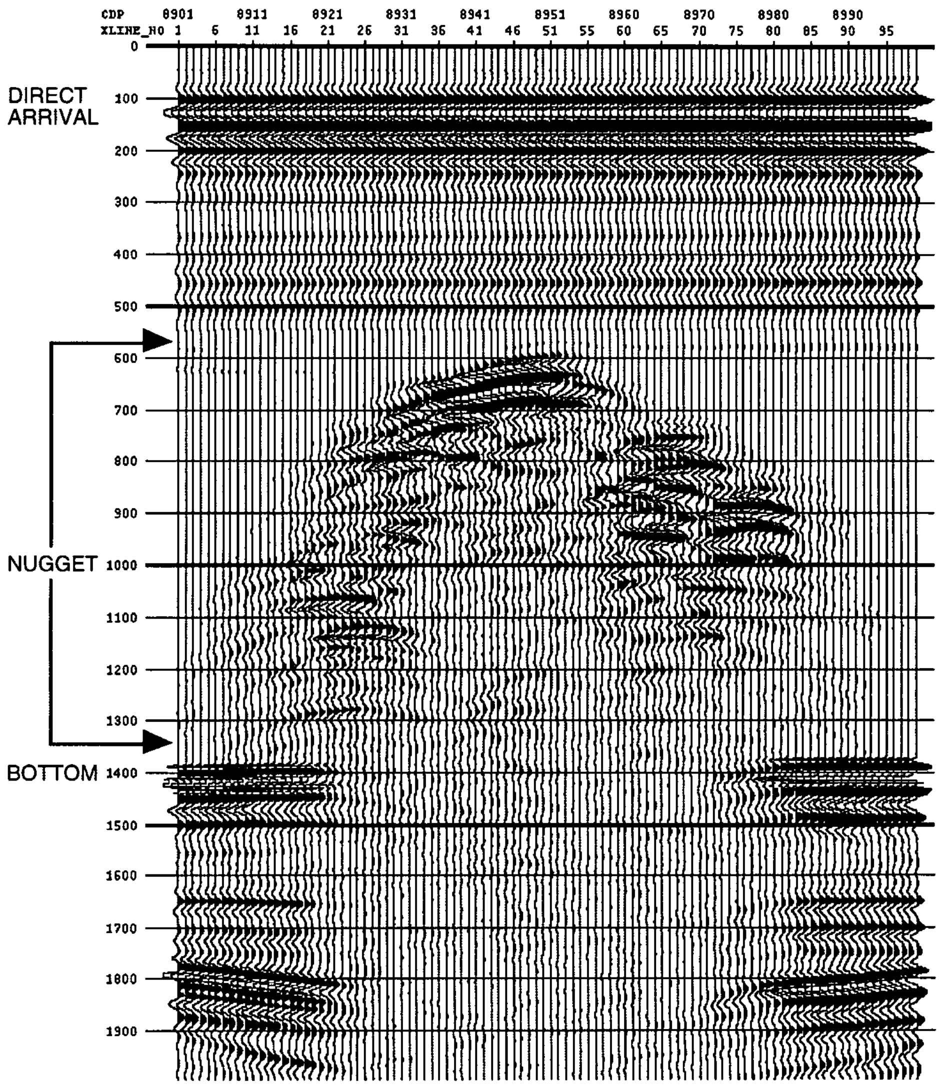

FIG. 5. Inline 90 from the raw data. See Figure 3 for location. The data was cropped to a maximum sample length of 1995ms. The data have also been bandpassed filtered to eliminate noise. No AGC was applied.

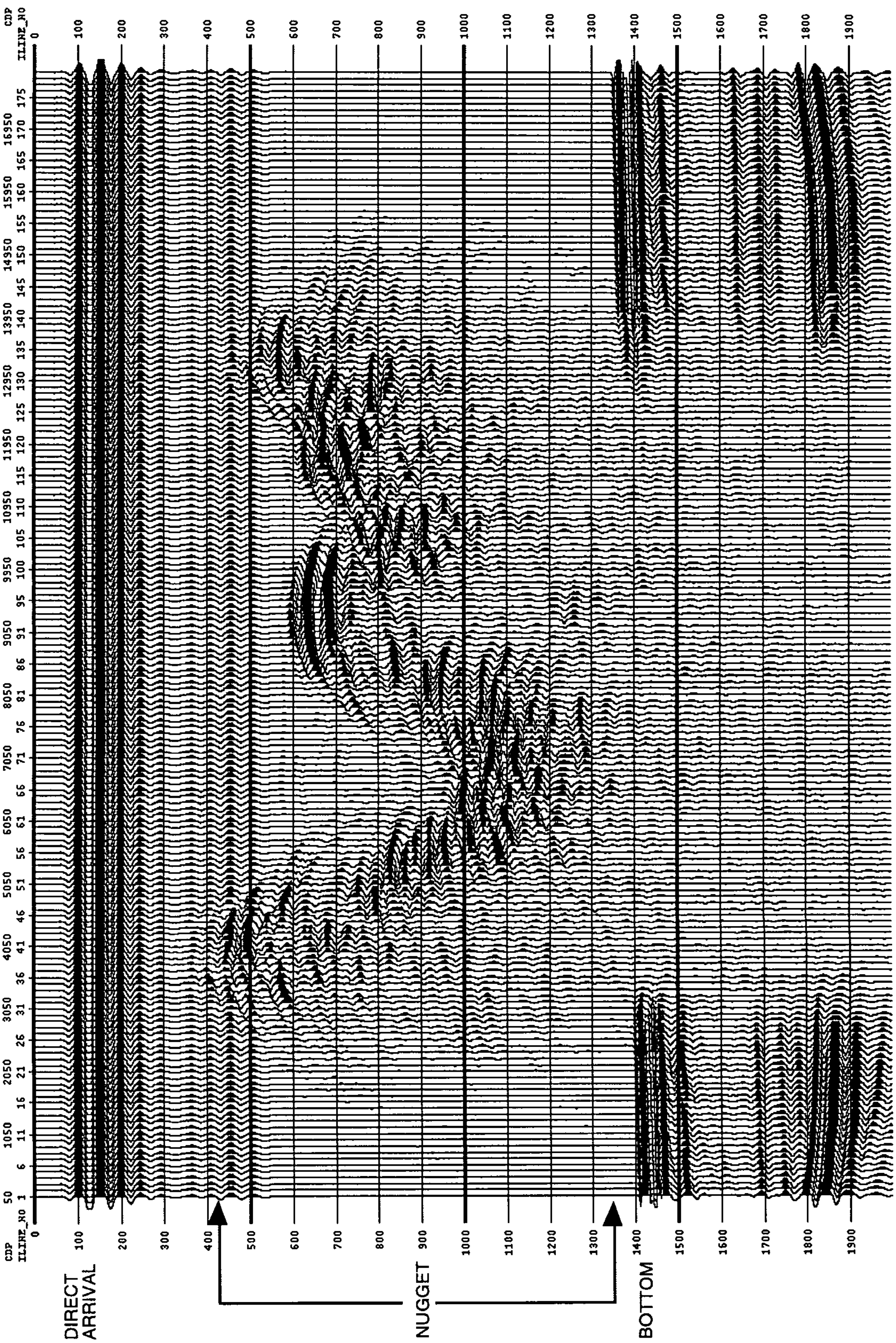

Fig. 6. Crossline 50 from the raw data. See Figure 3 for its location. This data was treated in the same manner as Inline 90 (Figure 5).

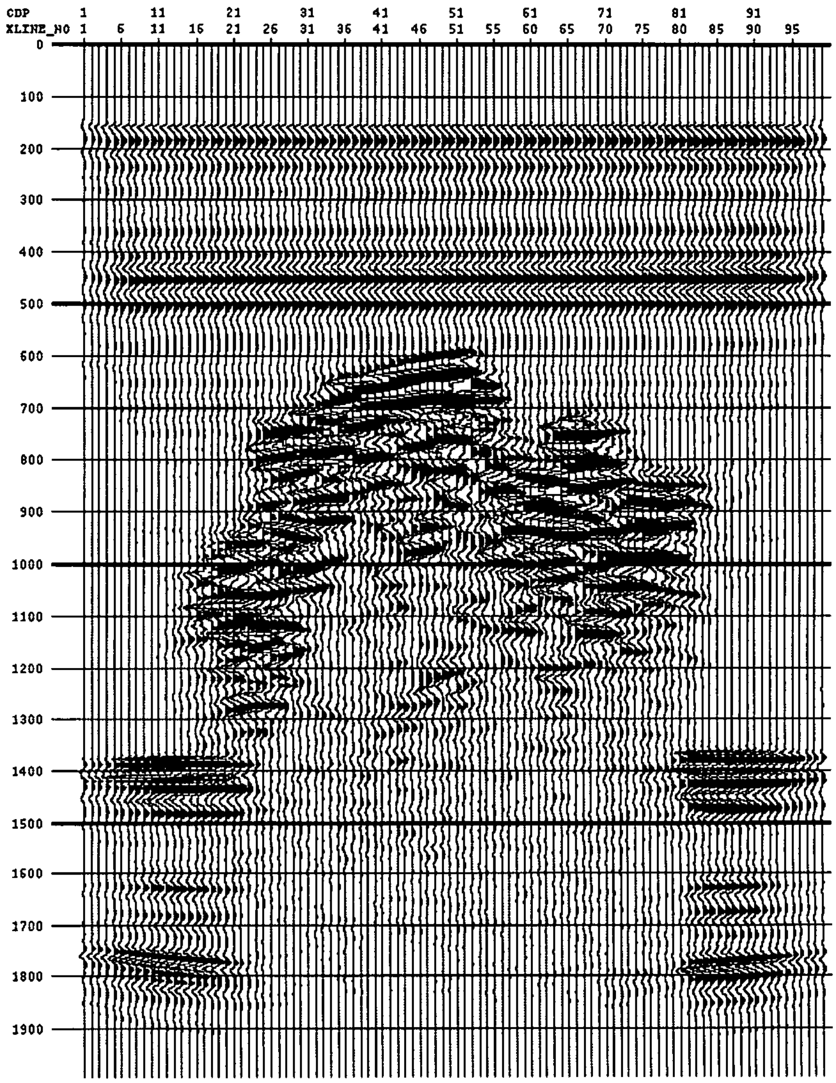

Fig. 7. Inline 90 after time migration has been applied. It shows the width of the nugget to be approximately 13cm (in unscaled dimensions).

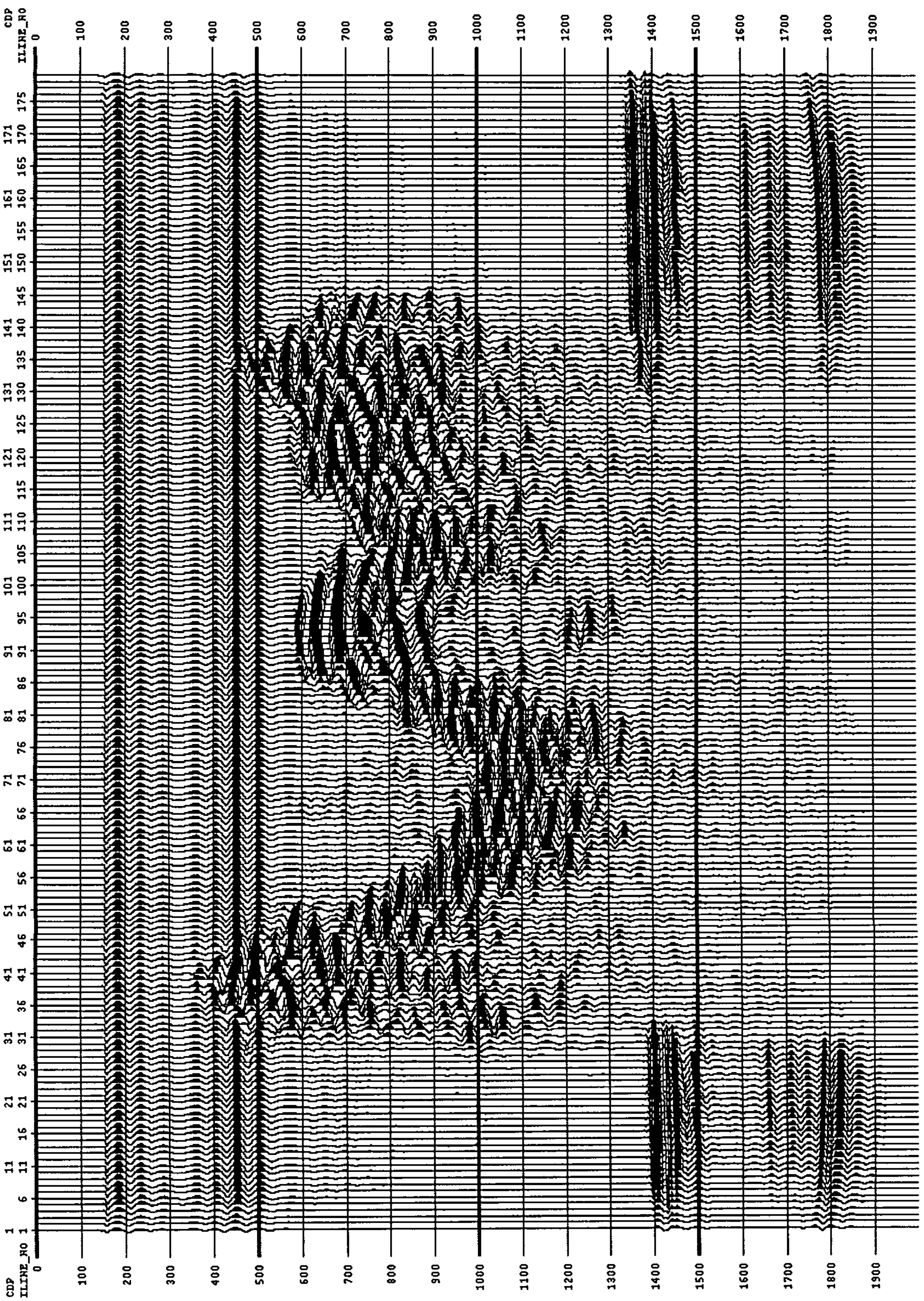

Fig. 8. Crossline 50 after time migration has been applied. It shows the length of the nugget to be approximately 23cm and the height of the nugget to be 7.5cm at the highest point (dimensions not scaled).